Operational Soil Stiffness from Back-Analysis of Pile Load Tests within Elastic Continuum Framework

Fawad S. Niazi[1] and Paul W. Mayne[2]
School of Civil and Environmental Engrg., Georgia Institute of Technology, Atlanta, Georgia, USA
[1]*E-mail*: fniazi6@gatech.edu
[2]*E-mail*: paul.mayne@gatech.edu

ABSTRACT: New sets of shear stiffness reduction curves are developed from the back-analyses of 299 static axial pile load tests from 61 sites towards the implementation of a non-linear load-displacement (Q-w) response method for pile foundations. The initial shear modulus (G_{max}) is derived from the measured shear wave velocity (V_s) profiles at the pile sites, usually obtained from seismic cone penetration tests (SCPT). A Randolph-type closed-form elastic continuum solution for axial compression loading is used, modified for additional applications involving axial tension loading cases. The back-analysis of shear moduli at various load levels results in derivations of new shear modulus reduction curves, specifically normalized shear stiffness (G/G_{max}) vs. logarithm of pseudo-strain: $\gamma_p = w_t/d$, where w_t = pile top displacement and d = pile diameter. These curves incorporate the effects of pile type and installation method, and also show the influence of soil plasticity. A complete step-by-step methodology is presented for use and application of these new stiffness reduction curves within the extended system of closed-form elastic continuum solutions. In a companion paper, these solutions are further extended towards their application to a stacked pile model, representing certain practical field situations of non-homogeneous and non-Gibson type soil profiles, and accounting for the concept of progressive failure with depth.

KEYWORDS: Pile foundations, Displacements, Load tests, Shear modulus, Shear wave velocity, Soil stiffness, Plasticity index

1. INTRODUCTION

The nonlinear response of geomaterials to loading has been widely researched and documented towards use in geotechnical engineering applications (Burland 1989). The mechanical non-linearity is exhibited in the form of soil stiffness that begins at the small-strain shear modulus (G_{max}) and softens when shear strains (γ_s) exceed the linear threshold value, resulting in marked reductions for small, intermediate, and large strains until the shear strength is reached (Tatsuoka and Shibuya 1992). Many algorithms have been developed to describe this stiffness reduction for soils, including: hyperbolic stress-strain relationships, power law expressions, spline functions, and periodic logarithmic functions, as well as constitutive soil models based on elasto-plasticity (Mayne 2005). It becomes difficult to strike a compromise between simplicity, without regard for imprecise description of rather complicated stiffness reduction trends, and improved accuracy which is attained at the cost of highly complex algorithms.

The operative soil shear stiffness (G) is the most important parameter affecting the response of deep foundations in terms of displacements resulting from the applied loads, starting from an initial value and leading up to the ultimate pile capacity under working conditions (Cooke et al. 1979). The nonlinear axial pile load vs. displacement (Q-w) analysis can be performed via several approaches, including: (a) elastic continuum solutions; (b) spring models (e.g., τ-z curves and q-z curves), (c) numerical simulations (e.g., finite elements, finite differences), or (d) empirical approaches. The evaluation of the initial shear modulus (G_{max}) in the range of strains less than the linear threshold becomes paramount. Elhakim (2005) showed that the in-situ seismic tests provide much more definitive and reliable means of assessing G_{max} compared to that obtained from laboratory tests. This fundamental stiffness can be conveniently obtained from in-situ measurements of shear wave velocity (V_s) during seismic cone penetration tests (SCPT or SCPTu): $G_{max} = \rho_t V_s^2$, where ρ_t = soil mass density.

For over 4 decades, the resonant column (RC) device has provided modulus reduction data for dynamically-loaded soils (e.g., Hardin and Drnevich 1972; Ishibashi-Zhang 1993; Santos and Correia 2001). The emphasis of measurement was to define G_{max} and the associated normalized operative shear stiffness (G/G_{max}) reduction curves at small to intermediate strains, as well as damping values (e.g., Vucetic and Dobry 1991). It is important to note that the rates of loading are quite high for RC tests, thus these G/G_{max} schemes are not directly appropriate to static monotonic load testing of pile foundations.

Vucetic and Dobry (1991) identified plasticity index (PI) as a major factor affecting the G/G_{max} reduction curves for a wide variety of geomaterials. Consequently, design charts showing modulus reduction curves as function of PI were developed. Their use, however, is more appropriate to seismic site amplification studies and cyclic behavioral concerns (Elhakim 2005). Moreover, the trends were not expressed mathematically for convenient use of the G/G_{max} vs. logarithm of γ_s relationships.

Berardi and Bovolenta (2005) proposed a semi-empirical approach of matching field measurements via back-analysis of pile load tests using analytical elastic solutions. This procedure enables the derivation of G/G_{max} as a function of the pseudo-strain (γ_p), which can be defined as the ratio of pile top displacement to its diameter (w_t/d). Thus, they generated stiffness reduction curves based on actual field measurements from a limited database of similar pile situations (pile type, geometry, soil conditions, etc.) for loading in axial compression. The G values obtained from these curves can thus be used in the same elastic solutions to forecast the nonlinear load-displacement (Q-w) response of piles falling within the range of the database considered.

Recently, using laboratory experimental data from resonant column, triaxial, simple shear, and torsional shear tests on 21 clays and silts, Vardanega and Bolton (2011; 2013) presented a new scheme for estimating G for clays and silts, defined via G/G_{max} vs. γ/γ_{ref}. Here γ_{ref} refers to the value of γ where G_{max} reduces to one-half of its initial maximum value. They characterized their dataset by fitting a modified hyperbola via the following transformed system:

$$\log_{10}[(G_{max}/G) - 1] = \alpha \log_{10}(\gamma/\gamma_{ref}) \quad (1)$$

where the curvature parameter $\alpha = 0.763$ for static loading, and $\alpha = 0.943$ for dynamic loading. To explore the robustness of their relationship to γ_{ref}, regression analyses were performed on individual soil properties, thereby tying γ_{ref} to the PI of the soil via the following relationship:

$$\gamma_{ref} = J\,(PI/1000) \quad (2)$$

where, J = 2.2 for static loading and 3.7 for dynamic loading, and PI is expressed as numerical value, not as a percentage. Accordingly, they presented new PI based curves similar to the Vucetic and Dobry (1991) type charts for both dynamic and static loading for clays and silts, along with their respective design equations. The new curves of static loading are displaced from the Vucetic and Dobry (1991) curves indicating a less stiffer and earlier yielding response than dynamic loading. This is a clear manifestation of the phenomenon of interpretation of higher stiffness response for increased strain rate due to soil viscosity (e.g., Garner 2007). It provides motivation for introduction of adjustment factors in the G/G_{max} reduction schemes derived from cyclic and dynamic loading towards static application, or derivation of separate G/G_{max} reduction scheme for use in static loading of pile foundations.

In this study, a framework has been established which combines two approaches: (a) back-figured moduli from load tests normalized to field G_{max} measurements (Berardi and Bovolenta 2005), and (b) modified hyperbolic fitting of the corresponding G/G_{max} reduction curves vs. logarithm of shear strains (Vardanega and Bolton 2011; 2013). This represents an effort to develop a set of modulus reduction curves from the back-analyses of a large number of pile load tests conducted in a broad assortment of geomaterials. The retro-investigation has been performed within the framework of analytical elastic continuum solutions by Randolph (2007). In addition to the tests performed under conventional axial compression loading, this database also encompasses piles load-tested in uplift (or tension). This paper explains how the elastic solutions were de-coupled and modified for adaptation to tension loading cases and subsequently used to back-figure operational stiffnesses for both compression and tension cases. New charts have been developed presenting design curves and their affiliated algorithms for different pile types and soil conditions to be utilized for axial pile Q–w analysis within this elastic continuum framework.

2. ELASTIC CONTINUUM SOLUTIONS

2.1 Review

An analytical elastic solution for pile-soil interaction, representing the Q-w relationship for single pile foundations, originally proposed by Randolph and Wroth (1978; 1979), exists in its latest form in Randolph (2007). It was developed for piles loaded in top-down axial compression mode, embedded in a linear elastic two-layered soil model with the boundary lying at the pile tip elevation (see Figure 1, where different terms of the solutions are also explained).

This analysis assumes elastic stiffness properties for the soil layers. Furthermore, the initial solutions employ simplifying assumptions, such that responses of pile shaft and tip are first treated separately, i.e., the settlements around the pile shaft are due to the shaft load, and those of the tip are due to tip load only, and that the pile material is stiff enough to render pile as rigid [i.e., for any load applied at the pile top (Q_t), the settlements are same all along the pile length, including top-settlements (w_t) and tip-settlements (w_b)]. These solutions were then modified by incorporating appropriate considerations to account for the pile compressibility, thereby allowing for the assessments of separate settlements at the pile top and tip for compressible piles. The modifications were applied by introducing the measure of pile compressibility (μL), and the pile-to-soil stiffness ratio (λ) factor.

While the solutions are quite versatile, they still carry following limitations:

- The original solutions do not explicitly account for the non–linear soil stiffness softening at increasing loads. This creates principal difficulty in the selection of elastic stiffness properties of soil for use in these solutions to estimate settlements corresponding to varying levels of load.
- These solutions cannot be applied directly to the case of piles subjected top-applied axial tension (or uplift loading), without appropriate modifications.
- Effects of differences in the pile types and installation methods (i.e., driven vs. jacked vs. bored vs. augered) on the axial load response are not explicitly addressed in the solutions.
- Not all field situations present simple homogeneous soil profiles (where modulus is constant with depth) or general Gibson soil types (where modulus increases linearly with depth) for which the solutions were derived, thus warranting appropriate modifications to account for alternative soil models.
- The model does not account for the concept of progressive failure with depth where the shaft resistance mobilizes prior to base resistance, as identified in pile load tests.

Despite the above constraints, inherent in these solutions are certain provisions such that their exploitation provides a recipe for improved performance of this analytical method. While this paper presents modifications to account for tension loading, and offers new stiffness reduction charts to be used for applicable working loads for different pile types and soil characteristics, its companion paper addresses the issues related to oversimplification of soil profiles as homogeneous or Gibson type, and incorporates the concept of progressive failure with depth.

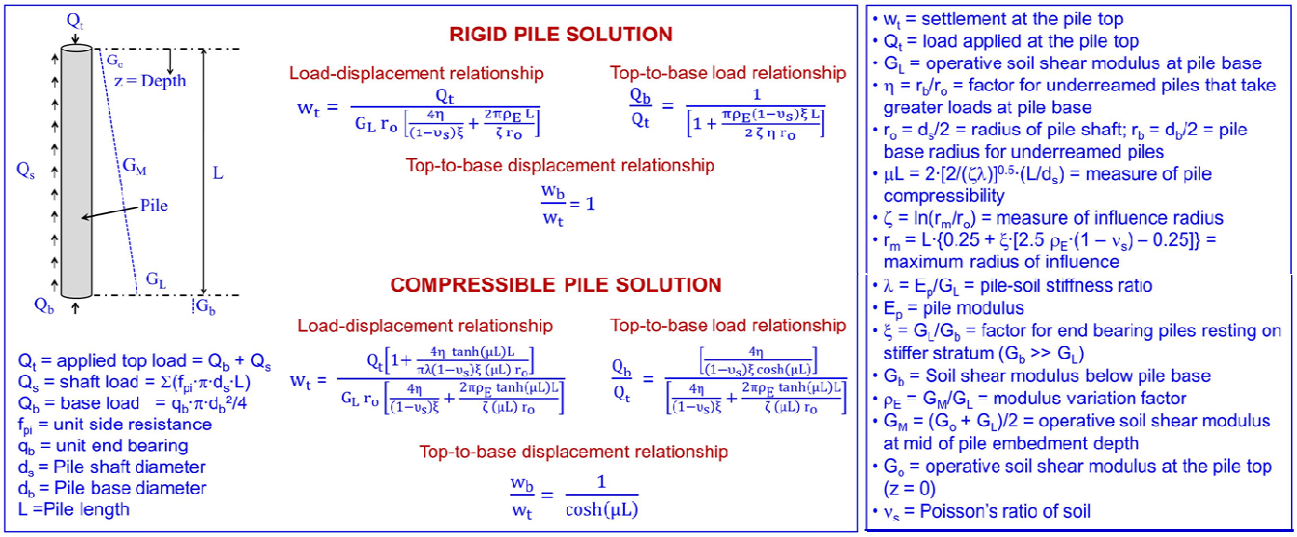

Figure 1 Analytical elastic continuum solution for axial pile displacements analysis in a linear elastic two layered soil model (adapted after Randolph and Wroth 1978; 1979; Randolph 2007).

2.2 Modification for Tension Loading

To extend this model to top-applied tension (or uplift) loading cases, the following observations need consideration:

- A test pile which is loaded in uplift has the load applied to the pile shaft by a system pulling upward at the top, thus placing the foundation into tension.
- The Poisson's ratio effect due to elastic deformation of the pile material for tension case tends to reduce the lateral stress at the pile-geomaterial interface, whereas the opposite occurs for the case where the shaft is loaded in compression.
- Previous research studies concluded that the reported range of tensile to compressive shaft capacity ratio [$\theta_{t/c} = Q_{s(t)}/Q_{s(c)}$] spans between 0.50 and 0.90, with an overall average value of 0.70. The results of a recent research effort by the authors on a database of 153 pile load tests from 52 sites in 17 different countries of the world indicate that the ratio $\theta_{t/c}$ averages 0.763 (Niazi and Mayne 2013).
- In tension loading, shaft resistance (Q_s) is the primary component of axial pile capacity. It implies that the base resistance component (Q_b) may not activate in case of tension loading. This could be true for the drained loading case where the pile foundation is embedded in coarse grained soils. However, for piles installed in silts and clays, undrained conditions exist, whereby suction effects at the pile tip may generate a small component of Q_b in downward direction. McManus and Kulhawy (1994) reported from test measurements during cyclic axial loading of a drilled shaft in "Cornell clay" that excess pore water pressures (Δu) up to one atmosphere (σ_{atm} = 100 kPa) may be generated at the pile tip.

To account for the above factors, following modifications are proposed to the Randolph closed form pile solutions for the case of tension loading (also see Figure 2).

2.2.1 Piles Embedded in Sand

The tension load applied at the pile top (Q_t) is resisted by two components: (1) a reduced shaft resistance in tension [$Q_{s(t)}$] along the pile length; and (2) the pile buoyant weight (W). Accordingly, the mathematical expression for tension load in case of piles embedded in sand reduces to the following form:

$$Q_t = Q_{s(t)} + W = \theta_{t/c} \cdot Q_{s(c)} + W = \theta_{t/c} \cdot \Sigma(f_{p(c)} \cdot 2\,\pi\, r_o \cdot L) + W \qquad (3)$$

where, $\theta_{t/c}$ is the ratio of tensile to compressive pile shaft capacity averaged at 0.763, $Q_{s(t)}$ = shaft capacity in tension, $Q_{s(c)}$ = shaft capacity in compression, $f_{p(c)}$ = unit shaft resistance in compression, r_o = shaft radius, W = pile buoyant weight, L = pile length. As seen, the term for pile base resistance (Q_b) has been neglected. Similarly, omitting the applicable terms, i.e., $4\eta/[(1 - \nu_s)\xi]$, in the numerator and denominator terms that relate to the base contribution, the elastic solution reduces to the form shown below:

$$w_t = \frac{Q_t\, \zeta\, (\mu L)}{2\pi \rho_E\, G_L \tanh(\mu L) L} \qquad (4)$$

Various terms in the above equation have been defined previously in Figure 1 and are reproduced in Figure 2 for completeness.

2.2.2 Piles Embedded in Clay and/or Silt

In case of piles installed in fine-grained soils, the tension load applied at the pile top (Q_t) is resisted by 3 components: (1) a reduced shaft resistance [$Q_{s(t)}$] along the pile length; (2) pile buoyant weight (W); and (3) a nominal resistance at the pile base (Q_b) because of possible suction effects from the change in pore water pressure generated beneath the pile tip. This is mathematically expressed as:

$$\begin{aligned} Q_t &= Q_{s(t)} + W + Q_b = \theta_{t/c} \cdot Q_{s(c)} + W + Q_b \\ &= \theta_{t/c} \cdot \Sigma(f_{p(c)} \cdot 2\,\pi\, r_o \cdot L) + W + q_b \cdot A_b \\ &= \theta_{t/c} \cdot \Sigma(f_{p(c)} \cdot 2\,\pi\, r_o \cdot L) + W + \Delta u \cdot \pi r_b^2 \end{aligned} \qquad (5)$$

where, $Q_{s(t)}$ = shaft capacity in tension, $Q_{s(c)}$ = shaft capacity in compression, $f_{p(c)}$ = unit shaft resistance in compression, r_o = shaft radius, W = pile buoyant weight, L = pile length, q_b = unit base resistance, A_b = cross-sectional area of pile tip, Δu = measured change in pore water pressure (ranging between zero and σ_{atm} = 100 kPa, depending on the drainage characteristics of the soil at the pile tip), and r_b = pile base radius. Since certain base resistance component forms part of the total resistance in the case of fine-grained soils, the original expression of the closed form elastic solution with terms for the base resistance is still applicable:

$$w_t = \frac{Q_t\left[1 + \frac{4\eta\, \tanh(\mu L) L}{\pi\lambda(1-\upsilon_S)\xi\, (\mu L)\, r_o}\right]}{G_L\, r_o \left[\frac{4\eta}{(1-\upsilon_S)\xi} + \frac{2\pi\rho_E \tanh(\mu L) L}{\zeta\, \mu L\, r_o}\right]} \qquad (6)$$

All terms in the above equation have been defined previously in Figure 1 and are also reproduced here in Figure 2.

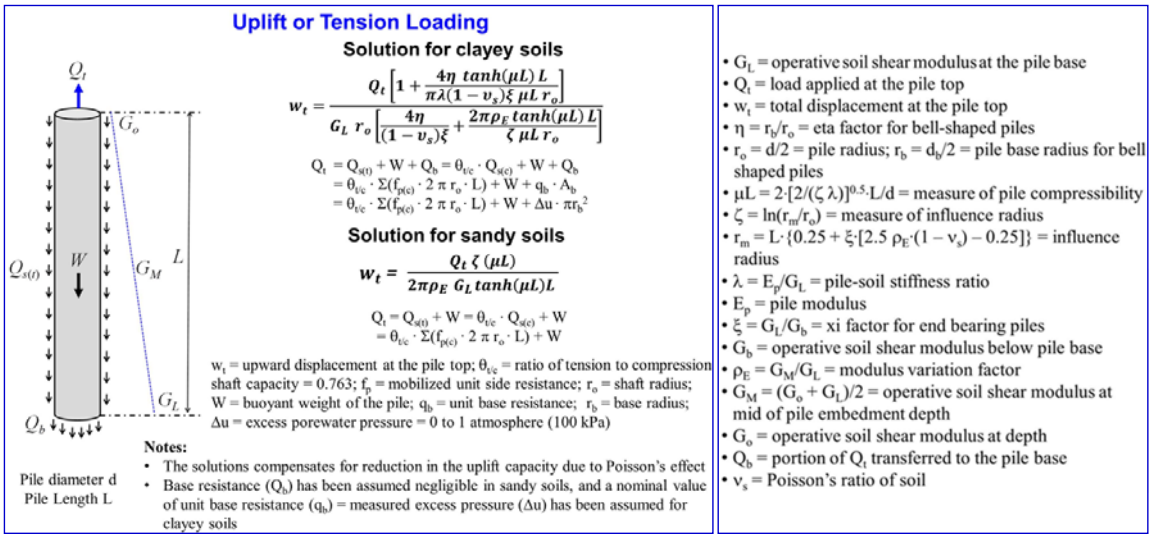

Figure 2 Elastic pile solution for estimating upward displacements for axial tension loading.

3. BACK-ANALYSIS OF SHEAR MODULI FROM PILE LOAD TESTS

3.1 Database of Pile Load Tests

A database of 299 pile load tests at 61 sites from different parts of the world was compiled that provide Q-w data as well as the V_s readings.

The load tests include the conventional compression (C) type: 203, and tension type (T): 96 arrangements, conducted on a wide variety of piles: drilled shafts (DS), square- and circular- concrete piles (Sq-C, Cir-C), open- and close-ended steel pipe piles (OE-S, CE-S), augered piles (A), H-section piles (HP), and wooden piles (Teak), installed in variety of geomaterials, ranging in overconsolidation ratio (OCR) from 1 to 40, and non-plastic (NP) soils (i.e., sands) as well as low to highly plastic soils (i.e., silts and clays) with PI values ranging from 5 to 105. The piles in the databank vary greatly in diameter (or width) as well as length. More than 85% of the piles have diameters within the range of 0.04 m to 0.915 m, with an overall mean of 0.56 m. Similarly, about 88% of piles have lengths ranging between 2.15 m and 35.0 m, with overall mean of 15.5 m. For non-circular piles (Sq-C and HP), equivalent shaft diameters were calculated from their outer perimeters, based on the recommendations by Seo et al. (2009). A concise summary of the case records, presenting information on the site names and locations, soil profiles, pile types/materials, pile installation methods, pile loading modes, and number of load tests at each site, is provided as a supplemental data in electronic form.

For predominant majority of these sites (54 sites), the V_s reading were acquired from SCPT or SCPTu. For some (4 sites), V_s data were available from alternative investigation methods [e.g., seismic dilatometer test (SDMT), spectral analysis of surface waves (SASW), and/or conventional downhole test (DHT)], while well-established correlations were used for the remaining 3 sites, where the pile load test data were very well documented.

3.2 Back-analysis Methodology

A scheme of back-analyses of operational shear stiffnesses was formulated similar to the approach adopted by Berardi and Bovolenta (2005). Accordingly, eqs. (4) and (6) were rearranged to the following forms:

$$G_L = \frac{Q_t\,\zeta\,(\mu L)}{2\pi\rho_E\, w_t \tanh(\mu L) L} \tag{7}$$

$$G_L = \frac{Q_t\left[1+\frac{4\eta\,\tanh(\mu L)L}{\pi\lambda(1-\upsilon_S)\xi\,(\mu L)\,r_o}\right]}{w_t\, r_o\left[\frac{4\eta}{(1-\upsilon_S)\xi}+\frac{2\pi\rho_E\tanh(\mu L)L}{\zeta\,(\mu L)\,r_o}\right]} \tag{8}$$

Further specifics on the methodology of the current retro-investigation are detailed below:

- Equation (7) applies to the cases of tension load tests in sand, while eq. (8) was used for the cases of compression load tests as well as those of tension load tests in clays and silts.
- The applied loads (Q_t) and their corresponding measured displacements (w_t) from each load test were used in the above equations, duly incorporating expressions (3) and (5) on case-to-case basis.
- The remaining input parameters required for these solutions were adopted from the information obtained from their respective data sources at these sites. Accordingly, the pile moduli (E_p), required for calculating the pile-soil stiffness ratios ($\lambda = E_p/G_L$) and the measure of pile compressibility (μL) were implemented. For other situations, where this information was not available, appropriate values from similar pile types were assumed.
- The G_{max} profiles and the related ρ_E factors obtained via V_s measurements mostly indicated either relatively uniform conditions or general Gibson soil types.
- For the soil Poisson's ratio (ν_s) values, the following assumptions were made: drained conditions for predominantly sandy soils (ν_s = 0.20), while undrained conditions for predominantly clayey soil layers (ν_s = 0.50). However, where this information was explicitly given in the original data source, the reported values were adopted.
- Inherent in this framework of back-analysis are the following two assumptions that are reasonably acceptable from an engineering point of view: (1) the stiffness is linearly dependent on the depth, although some real situations may portray a different trend, and (2) the back-analyzed field stiffness can be obtained keeping ρ_E constant, i.e., G along the shaft and at the base decrease at the same rate, although the shaft resistance is expected to mobilize prior to the end bearing.
- Hidden in the parameters on the right hand sides of eqs. (7) and (8) is the input of G_L. A trial and error method (or a computer program capable of running the required iterations) can be used to match the values of G_L on both sides of the equation.

The operative shear stiffness (G) values so obtained and normalized via G/G_{max} as a function of $\gamma_p = w_t/d$ (%) provided the desired stiffness reduction trends.

3.3 Cumulative Results of Back-Analysis

The respective stiffness reduction curves from 299 pile load tests obtained via the selected back-analysis methodology were combined, as presented in Figure 3. As shown here, the pseudo-strain (γ_p) axis has also been normalized with respect to a reference pseudo-strain ($\gamma_{p\text{-}ref}$), taken as $w_t/d = 0.01$. This low value of $\gamma_{p\text{-}ref}$ has been adopted to match closely with the previous definitions of reference strain (γ_{ref}) found in the literature.

As clearly evident, the data points present a wide scatter. The database used herein is characterized by a wide variety of differing soil conditions, pile foundation types, and pile installation methods. Logically, such variability is not likely to derive consistent results in a combined plot, thus hampering its utilization in the development of modulus reduction algorithms which are suitable for future pile Q-w predictions. To facilitate some consistency towards development of modulus reduction algorithms, the results are shown in Figure 3 to have been sorted into groups based on pile typology and installation method. This sorting points to a certain hierarchical order in which the stiffness reduction trends may be ranked. In general, the drilled shafts which are installed using bored cast in-situ methods tend to present the most rapid reduction of the soil's operative shear modulus from its initial value of G_{max} in the range of percent γ_p (and even the normalized $\gamma_p/\gamma_{p\text{-}ref}$) < 0.1, beyond which the reduction becomes more gradual. On the other extreme, steel piles as well as precast concrete piles, installed using driven and jacked methods largely display the most gradual reduction of shear stiffness in the initial range of percent γ_p (< 0.1), becoming steeper for higher values. The auger piles fall in the intermediate category.

Despite these general observations, significant scatter still exists within each category, which may be attributed to additional characteristics of the soil deposits in the database. With PI-based trends of G/G_{max} vs. γ_s having already been established (e.g., Vucetic and Dobry, 1991; Vardanega and Bolton, 2011; 2013), it was considered reasonable to tap into the potential of exploring the effects of PI on this latest framework of G/G_{max} vs. $\gamma_p/\gamma_{p\text{-}ref}$, and then apply this approach to the pile response database in an analogous manner. Non-plastic soils (i.e., sands) were assigned a PI of zero, while cases involving fine-grained soils without plasticity information were omitted.

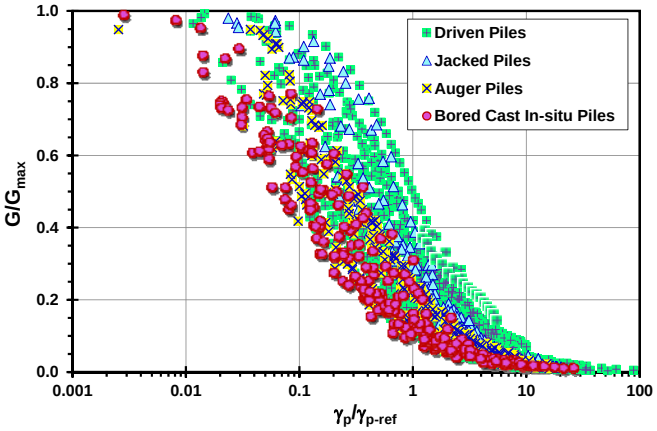

Figure 3 Sorted normalized operative shear stiffness vs. normalized pseudo-strain per the pile typology and installation methods.

3.4 Fitting a Model

It is evident from Figure 3 that the relationship between the predictor variable ($\gamma_p/\gamma_{p\text{-}ref}$) and the response variable (G/G_{max}) is nonlinear for different categories of pile type and installation. For such a relationship, it is advisable to work with alternative models where the variables are expressed after transformation. In order to linearly characterize the relationship for simple regression purposes, a modified hyperbolic model of the type similar to Vardanega and Bolton (2011, 2013) was fitted to the dataset of each pile category after transforming the response variable to the form ($G_{max}/G - 1$), and taking common logarithms of both predictor variable and the transformed response variable. The resulting plot is shown in Figure 4. A simple regression through the data points yields the following generalized and categorical correlations:

All Piles:
$$\frac{G}{G_{max}} = \frac{1}{\left[1+3.63\left(\frac{\gamma_p}{\gamma_{p-ref}}\right)^{0.94}\right]} \quad (9)$$

Driven Piles:
$$\frac{G}{G_{max}} = \frac{1}{\left[1+3.04\left(\frac{\gamma_p}{\gamma_{p-ref}}\right)^{1.01}\right]} \quad (10)$$

Jacked Piles:
$$\frac{G}{G_{max}} = \frac{1}{\left[1+2.36\left(\frac{\gamma_p}{\gamma_{p-ref}}\right)^{1.18}\right]} \quad (11)$$

Auger Piles:
$$\frac{G}{G_{max}} = \frac{1}{\left[1+4.28\left(\frac{\gamma_p}{\gamma_{p-ref}}\right)^{0.96}\right]} \quad (12)$$

Bored Piles:
$$\frac{G}{G_{max}} = \frac{1}{\left[1+6.95\left(\frac{\gamma_p}{\gamma_{p-ref}}\right)^{0.92}\right]} \quad (13)$$

To simplify the model, the following unified correlation is proposed to embrace the entire dataset on one end and to account for the pile installation method on the other end:

$$\frac{G}{G_{max}} = \frac{1}{\left[1+3.63\alpha1\left(\frac{\gamma_p}{\gamma_{p-ref}}\right)^{0.94\beta1}\right]} \quad (14)$$

where the values of coefficient $\alpha1$ and exponent $\beta1$ are parameters that, identify with the pile typology and installation methods, as presented in Table 1.

Table 1 Coefficients and exponents for G/G_{max} vs. $\gamma_p/\gamma_{p\text{-}ref}$ formulation (Eq. 14).

Pile classification (type/installation method)	**α1**	**β1**
Driven	0.84	1.07
Jacked	0.65	1.25
Auger	1.18	1.01
Bored Cast In-situ	1.91	0.97

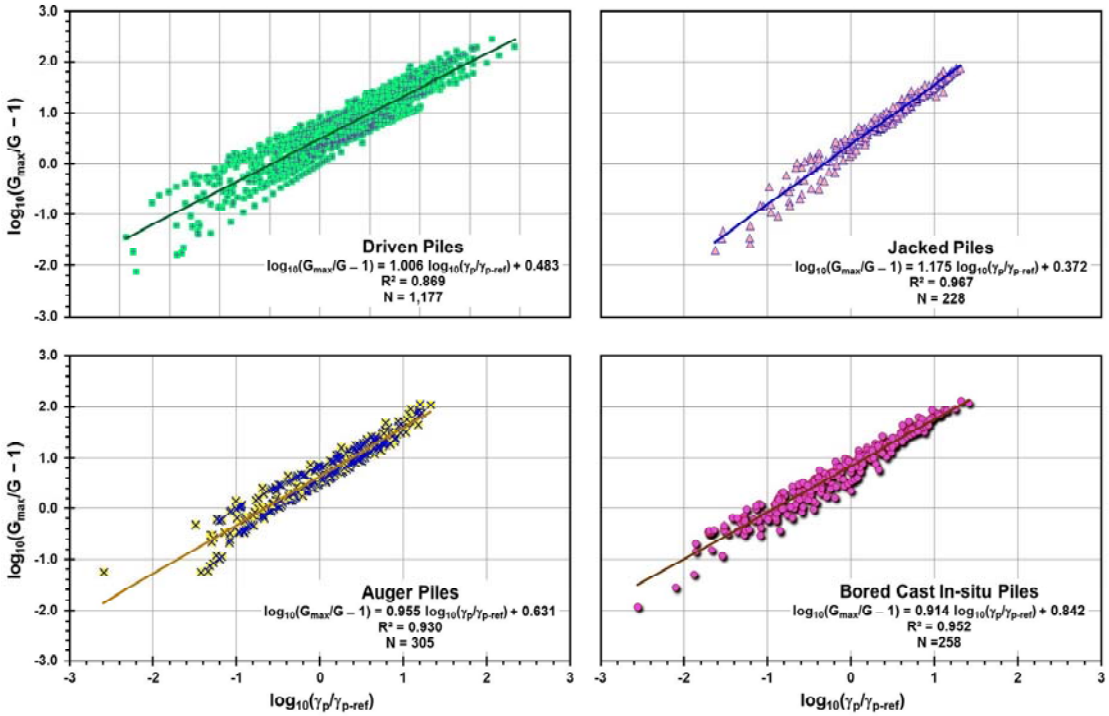

Figure 4 Modified hyperbola fitted to the transformed predictor and response variables of G/G_{max} vs. $\gamma_p/\gamma_{p\text{-}ref}$ formulation: (a) driven piles data; (b) jacked piles data; (c) auger piles data; (d) bored cast in-situ piles data.

To mitigate the scatter within each category of piles in an effort of further refinement of the model, it was considered prudent to incorporate the influence of PI in the new design formulation. Therefore, the data were additionally sorted based on the soil plasticity information. Accordingly, the slopes and intercepts from linear regressions of the transformed predictor and response variables were obtained for different PI values within each category of piles. The reverse transformation of these linear regression fitting models resulted in additional sets of coefficients and exponents ($\alpha 2$ and $\beta 2$) that present the effect of PI. Equation (14) thus takes the following form:

$$\frac{G}{G_{max}} = \frac{1}{\left[1+3.63\ \alpha 1\ \alpha 2\left(\frac{\gamma_p}{\gamma_{p-ref}}\right)^{0.94\ \beta 1\ \beta 2}\right]} \quad (15)$$

Subsequently, separate graphs were plotted for each pile category with percent PI values on the abscissa axis while $\alpha 2$ and $\beta 2$ on the ordinate axis. Different fitting functions were explored to define the trends, followed by superimposing the outcome of these functions on the original datasets. The hyperbolic tangent function delivered better results of this superimposition. The plots of these functions are shown in Figure 5. The use of hyperbolic tangent function offers an added advantage of limiting the upper and lower values of the curve fitting coefficient $\alpha 2$ and exponent $\beta 2$, restraining the predicted values from being non-representative near the outer bounds of the dataset, and thereby providing improved fitting.

In summary, the two sets of coefficients ($\alpha 1$ and $\alpha 2$) and exponents ($\beta 1$ and $\beta 2$) of eq. (15), identifying the effects of pile typology/installation methods, as well as the influence of PI on G/G_{max} vs. $\gamma_p/\gamma_{p\text{-}ref}$ formulation for the two proposed hyperbolic tangent fitting function are presented in Table 2.

4. NEW DESIGN CHARTS

For convenience and ease in application, it is considered reasonable to present these new design formulations in graphical form. Moreover, the abscissa axis can be simplified to percent pseudo-strain [i.e., γ_p (%)] instead of normalized pseudo-strain ($\gamma_p/\gamma_{p\text{-}ref}$), as the numerical values of both are same because of the selected reference strain [$\gamma_{p\text{-}ref}$ (%) = 1.0]. Accordingly, a set of design charts have been prepared for the four categories of piles (see Figure 6). These charts also show their respective design equations pertaining to the pile type and those for estimating their respective coefficients $\alpha 2$ and exponents $\beta 2$ which integrate the influence of PI on shear modulus reduction.

The general trends appear consistent with both the earlier Vucetic and Dobry (1991) charts and the recent Vardanega and Bolton (2011; 2013) design charts and equations. A direct simple apple-to-apple comparison is, however, not possible for the fact that the strain values taken in the current analysis have been defined on the basis of relative pile displacements (w_t/d), termed here as pseudo-strains (γ_p), in contrast to the classical strain definitions given for laboratory shear tests. The reference strain at $w_t/d = 0.01$ (used for normalization, i.e., $\gamma_p/\gamma_{p\text{-}ref}$) is also different from the one assumed by Vardanega and Bolton (2011; 2013), as well as other previous research works.

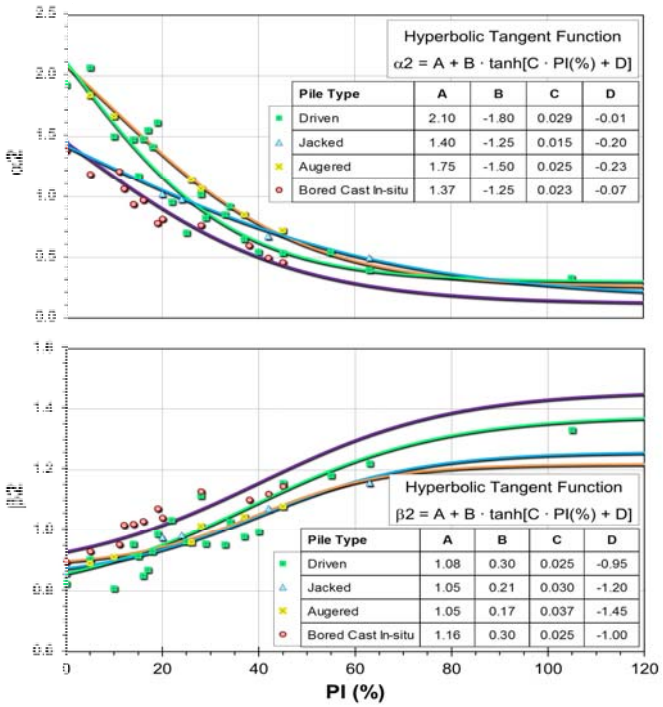

Figure 5 Correlations of coefficient $\alpha 2$ and exponent $\beta 2$ with plasticity index: hyperbolic tangent fitting function.

5. ASSESSMENT OF NEW DESIGN FORMULATION

In order to test the performance of the newly-derived empirical functions, the predicted values of the normalized shear stiffness [$G/G_{max(predicted)}$] were plotted against their back-figured values [$G/G_{max(back\text{-}figured)}$] for the proposed function, as applied to the entire dataset. The underlying assumption of the following analysis is the conjecture that the back-figured values of shear modulus are representative of the field values, since these were derived from the actual load tests.

The results are presented in Figure 7, while Table 3 shows a summary of the basic statistics of the model. Simple linear regression analyses were conducted on the results to obtain the best fit line of the ratios of predicted to back-figured normalized shear stiffness, $[G/G_{max(predicted)}]/[G/G_{max(back\text{-}figured)}]$. The corresponding R^2 of these ratios were then calculated. Inspection of Figure 7 shows that the proposed function yields its trend line that ties near perfectly to the best fit line with an R^2 value of 0.975. As evident, more than 90% of the data fall within the $\pm$30% bounds. In Figure 7, some seemingly greater scatter for the G/G_{max} values < 0.25 pertain to the range of loading beyond commonly accepted pile capacity definitions. This scatter is consistent with the loss of accuracy at low G/G_{max} reported by Vardanega and Bolton (2013).

Following the comparative approach used by Jardine et al. (2005), Lehane et al. (2013), and Van Dijk and Kolk (2011), the mean value (μ) and the coefficients of variation (COV) of the ratios of $[G/G_{max(predicted)}]/[G/G_{max(back\text{-}figured)}]$ for the predictions made via the proposed formulation are discussed below:

Table 2 Coefficient and exponent values for G/G_{max} vs. $\gamma_p/\gamma_{p\text{-}ref}$ formulation via hyperbolic tangent fitting function (Eq. 15).

Pile type	$\alpha 1$	$\beta 1$	$\alpha 2$	$\beta 2$
Driven	0.84	1.07	2.1 – 1.8 ·tanh[0.03·PI (%) – 0.01]	1.1 + 0.3·tanh[0.03·PI (%) – 0.95]
Jacked	0.65	1.25	1.4 – 1.3·tanh[0.015·PI (%) – 0.2]	1.1 + 0.2·tanh[0.03·PI (%) – 1.2]
Auger	1.18	1.01	1.8 – 1.5·tanh[0.03·PI (%) – 0.23]	1.1 + 0.2·tanh[0.04·PI (%) – 1.5]
Bored cast in-situ	1.91	0.97	1.4 – 1.3·tanh[0.02·PI (%) – 0.07]	1.2 + 0.3·tanh[0.03·PI (%) – 1.0]

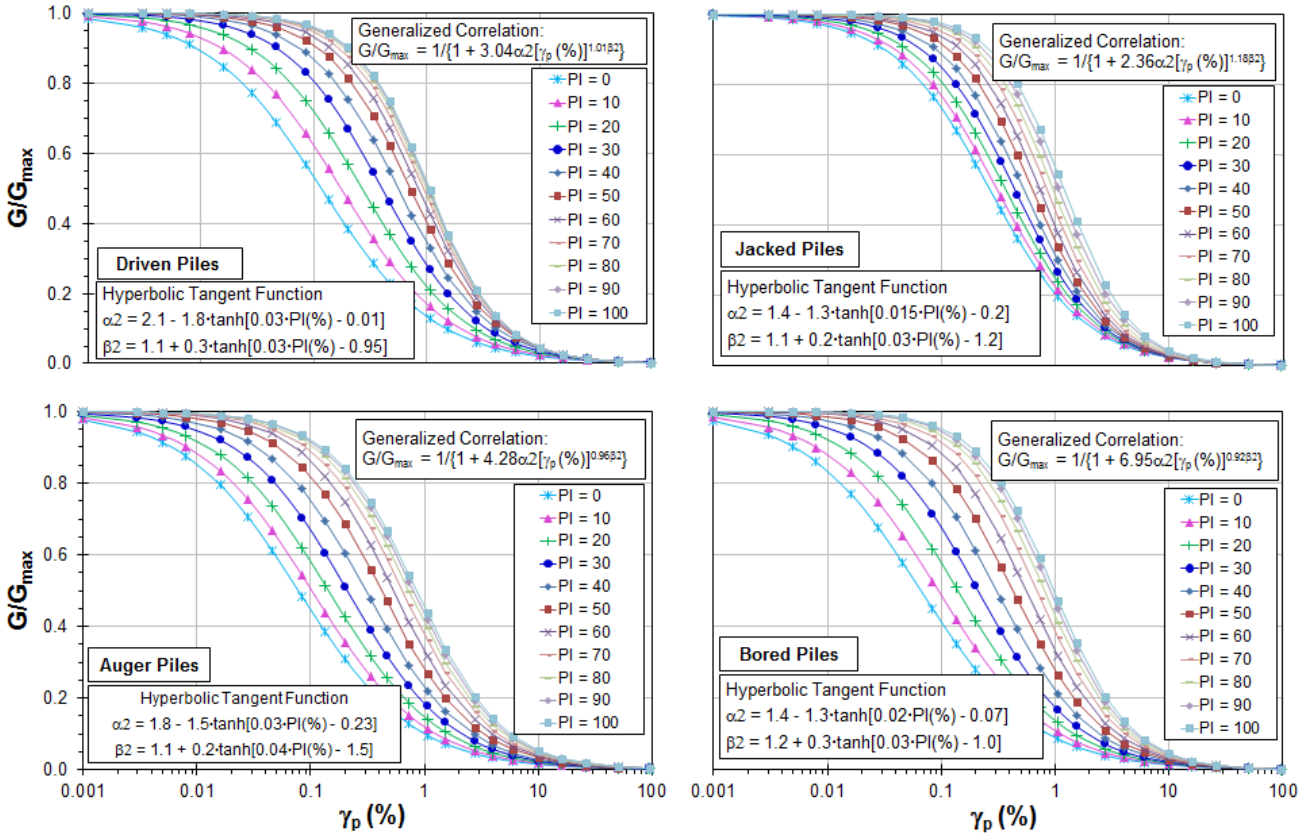

Figure 6 Design charts for shear stiffness reduction for application in the pile foundation analysis.

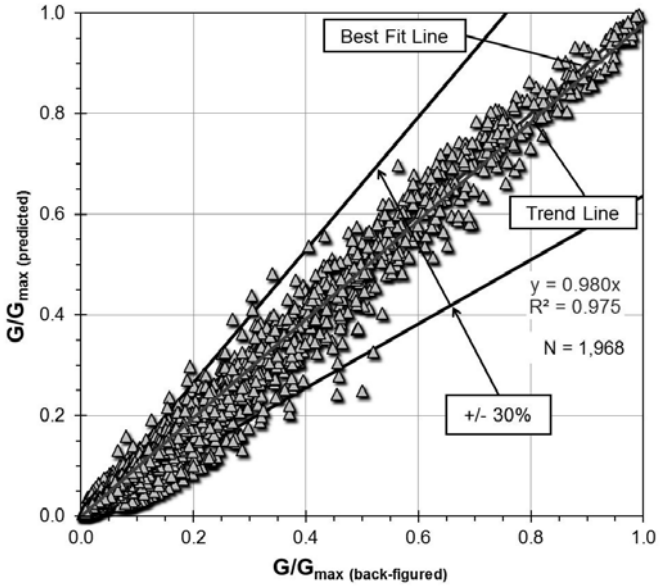

Figure 7 Predicted [$G/G_{max(predicted)}$] vs. back-figured [$G/G_{max(back-figured)}$] normalized shear stiffness.

- [$G/G_{max(predicted)}$]/[$G/G_{max(back-figured)}$] values display an approximately normal distribution, with μ = 0.944 and COV = 0.239. These value falls within a reasonable range for reliable predictions, and suggest an improved stiffness reduction model for a wide variety of piles and soils.
- With the assumption of a normal distribution for [$G/G_{max(predicted)}$]/[$G/G_{max(back-figured)}$], the μ value and COV of the new design formulation suggest a probability of 99.32% that the predicted normalized shear modulus [$G/G_{max(predicted)}$] will be less than 1.5 times the back-figured normalized shear modulus [$G/G_{max(back-figured)}$].
- To further evaluate the suitability and reliability of this model, it was subjected to additional assessments. Accordingly, the [$G/G_{max(predicted)}$]/[$G/G_{max(back-figured)}$] ratios were segmented into 5 zones of G/G_{max} values, namely, zone 1: 0 to 0.2, zone 2: 0.2 to 0.4, zone 3: 0.4 to 0.6, zone 4: 0.6 to 0.8, and zone 5: 0.8 to 1.0, followed by separate supplementary statistical analyses for each zone. The results are presented in Table 4. The moment statistics of the model (mean, standard deviation, minimum, maximum, range, variance, skewness, kurtosis) point to the following: (1) the distributions are narrow in zones 2 to 5 (i.e., the data points tend to be close to mean expected values), (2) the distributions are skewed slightly left of the mean values for zones 2 to 5, (3) the data in zone 1 present right skewed wide distributions. Accordingly, the accuracy is maximum in zones 3, 4, and 5, decreasing in zone 2, and least in zone 1. Despite this observed trend, the probability in zone 1 that the $G/G_{max(predicted)}$ will be less than 1.25 times the $G/G_{max(back-figured)}$ is 88.10%. This probability indicates increasing trends for zones 2, 3, and 4, with 100% for zone 5.

6. APPLICATION OF DESIGN CHARTS FOR PILE LOAD-DISPLACEMENT EVALUATIONS

The new sets of G/G_{max} vs. γ_p design charts can be used within the elastic continuum framework to predict loads (Q_t) for different values of displacements (w_t), so as to derive their complete non-linear Q-w curves. The methodology is summarized in the flow chart shown in Figure 8, and further detailed below:

- Collect information on pile dimensions (length, L and diameter, d) and pile modulus (E_p).
- Acquire downhole shear wave velocity (V_s) profile at the site. Here, downhole V_s has been preferred over alternative methods, since the stiffness reduction curves were developed using G_{max} values calculated from V_s readings obtained predominantly via downhole methods (mostly SCPT).

Table 3 Statistics of the hyperbolic tangent function model for G/G_{max} vs. γ_p.

Model Summary					
R	**R Square**	**Adjusted R Square**	**Std. Error of the Estimate**		
0.988	0.975	0.975	0.036		
ANOVA					
	Sum of Squares	**df**	**Mean Square**	**F**	**Sig.**
Regression	107.21	1.00	107.207	80847.34	0.000
Residual	2.62	1966.00	0.001	-	-
Total	109.82	1967.00	-	-	-
Coefficients					
	Unstandardized Coefficients		**Standardized Coefficients**	**t**	**Sig.**
	B	**Std. Error**	**Beta**		
Measured	1.003	0.004	0.988	284.337	0.000
(Constant)	-0.011	0.001	-	-9.282	0.000

Table 4 Statistics, G/G_{max} vs. γ_p (%) model for G/G_{max} values in Zones 1 to 5.

Statistics	**Zone 1: 0 to 0.2**	**Zone 2: 0.2 to 0.4**	**Zone 3: 0.4 to 0.6**	**Zone 4: 0.6 to 0.8**	**Zone 5: 0.8 to 1.0**
N	515	540	339	366	208
Mean	0.9342	0.9193	0.9861	1.0071	0.9923
Std. Error of Mean	0.0078	0.0087	0.0082	0.0059	0.0037
Median	0.9210	0.9295	1.0010	1.0160	0.9970
Mode	0.9120	0.9810	1.0460	1.0830	0.9770
Std. Deviation	0.2676	0.1723	0.1191	0.0689	0.0301
Variance	0.0716	0.0297	0.0142	0.0048	0.0009
Skewness	1.2085	-0.2575	-0.9034	-0.6711	0.0142
Kurtosis	6.8667	0.4496	2.2492	-0.0883	-0.0995
Range	2.818	1.000	0.824	0.303	0.140
Minimum	0.269	0.451	0.497	0.822	0.922
Maximum	3.087	1.451	1.321	1.125	1.062
Z-value at 1.25	1.180	1.919	2.217	3.524	8.548
$P[G/G_{max(predicted)} < 1.25\ G/G_{max(back\text{-}figured)}]$	88.10%	97.26%	98.67%	99.99%	100.00%

- From the V_s profile, determine the initial shear stiffness modulus profile ($G_{max} = \rho \cdot V_s^2$) with depth.
- From the G_{max} profile, obtain modulus values at mid-depth, at base of the pile, and below the base [$G_{M(max)}$, $G_{L(max)}$, and $G_{b(max)}$ respectively], and determine the stiffness variation factor [$\rho_E = G_{M(max)}/G_{L(max)}$].
- Select a value of displacement (w_t) and calculate the corresponding pseudo-strain [$\gamma_p = (w_t/d) \cdot 100$] as a percentage.
- Based on the pile type and installation method select the appropriate G/G_{max} vs. γ_p design charts. Using this chart, and from the average representative PI (%) of the soil along the pile length, calculate the coefficient $\alpha 2$ and exponent $\beta 2$.
- Using the same chart, calculate $G_L/G_{L(max)}$ from the applicable algorithm given in that chart, and thus obtain G_L value corresponding to the selected w_t.
- From the accepted assumption of this analysis, keeping ρ_E constant, i.e., G along the shaft and at the base decrease at the same rate, estimate the values of applicable G_M and G_b for the selected w_t.
- From E_p and G_L, calculate the pile-soil stiffness ratio ($\lambda = E_p/G_L$).

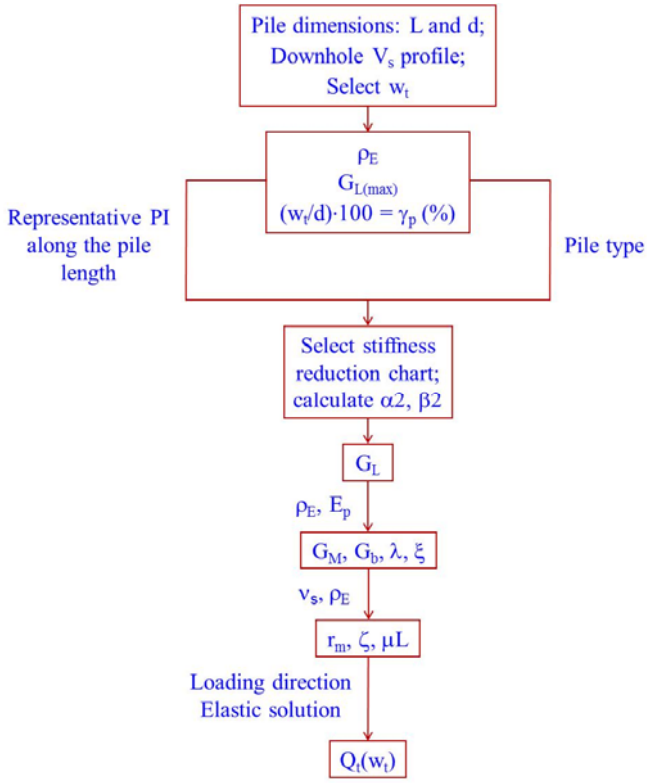

Figure 8 Flowchart detailing steps for estimating pairs of load-displacement values from the G/G_{max} vs. percent γ_p type design charts.

- Calculate ξ factor (= G_L/G_b) in case of end-bearing pile.
- From the soil Poisson's ratio (ν_s) and modulus rate parameter (ρ_E), calculate the maximum radius of influence {$r_m = L\,[0.25 + \xi\,(2.5\,\rho_E\,(1 - \nu_s) - 0.25)]$} and the measure of influence radius [$\zeta = \ln(r_m/r_o)$], where r_o is the shaft radius. In case of non-availability of ν_s information, use the previously noted assumptions: drained conditions for predominantly sandy soils ($\nu_s = 0.20$), and undrained conditions for predominantly clayey soil layers ($\nu_s = 0.50$).
- Calculate the pile compressibility {$\mu L = 2[2/(\zeta\lambda)]^{0.5}\,(L/d)$}.
- Depending upon the direction of loading and soil type at the site, use the following equations for estimating the load (Q_t) for the selected w_t: eq. (6) for the cases of compression loading as well as tension loading in clays and silts, and eq. (4) for tension loading in sands.
- Select different values of expected w_t and estimate their corresponding Q_t using the methodology described above.
- Draw complete Q-w curve for the selected pile and soil types.

From the details of this methodology, the solutions may seem to be relatively complicated. However, the solution presents a convenient set of equations that can be implemented into a spreadsheet with a minimal number of geotechnical input parameters (primarily soil stiffness profiles) to estimate the complete Q-w response of piles under axial compression and tension type of loadings.

6.1 Sample Calculations for a Case Study

In order to further elaborate on the specific procedural steps involved, sample calculations are presented for a 0.457-mm diameter, 32-m long close-ended driven steel pile, load-tested at the Wakota River Bridge site on I-494 Mississippi River Crossing in 2003. This replacement bridge was required to be constructed as a portion of the 6-year, 4-stage Minnesota Department of Transportation (MNDOT) I-494 and US 10/US 61 interchange reconstruction project.

The details of the project site, the related geotechnical information and the load testing program were obtained from Dasenbrock (2006). Only selected information is presented here, as related to its application in the proposed methodology. The site investigations initiated in year 2000 included SASW for acquisition of V_s data, and piezocone tests (CPTu) besides other field in-situ and laboratory testing to characterize the soil profile at the site. The subsurface conditions consist of layers of granular materials underlain by deposits of silty-clay over fine sand over clayey soils over dense sand over silty-loam spanning a total depth of 57 m. The V_s profile shown in Figure 9(a) was utilized to develop the small-strain (or fundamental) shear stiffness (G_{max}) profile of Figure 9(b). In order to define the variation of G_{max} as a function of depth, it is prudent to plot depth along abscissa and G_{max} along the ordinate (as presented in Fig. 9). The best-fit line forced through the data clearly indicates pure Gibson-type soil. Here, the soil unit weight, required for the calculations of G_{max} was estimated from the applicable correlations of CPTu from the literature. An overall average PI value from the available data was adopted at 25% for the pile length. A Poisson's ratio of 0.3 was assumed considering partially drained conditions for the overall soil profile.

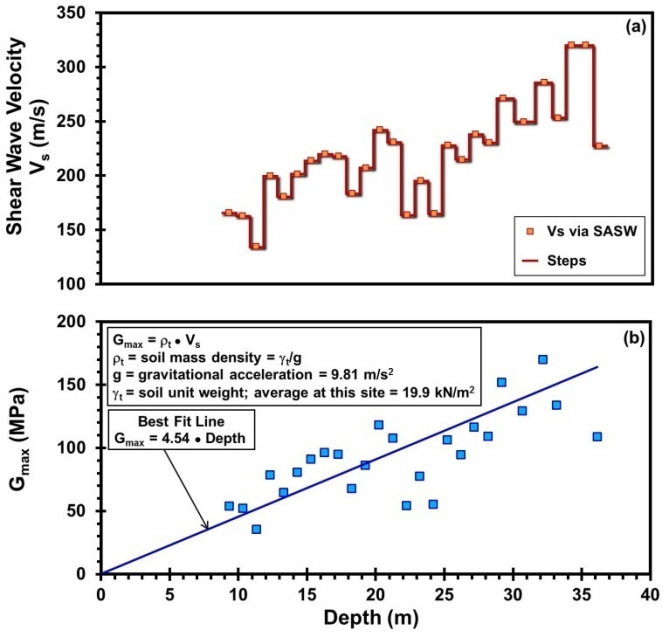

Figure 9 Shear wave velocity and shear stiffness profiles at Wakota River Bridge site on I-494 Mississippi River Crossing.

The pile elastic modulus was calculated while considering the pile wall thickness and adopting 200 GPa of approximate Young's Modulus for the steel material. The remaining parameters were all conveniently obtained and used in the spreadsheet calculations, as shown in Table 5. Here, eq. (15) in conjunction with Table 2 were used for calculating the operational shear stiffness (G_L) for selected top settlements (w_t), while eq. (6) in its rearranged form enable estimation of the corresponding loads at the pile top (Q_t). The predicted results of load-displacement response, as plotted against those of the measured from the load test in Figure 10 indicate a very good comparison.

Table 5 Sample calculations for the prediction of loads vs. selected settlements for a 32-m long, 0.457-m diameter closed-ended steel pipe pile from the proposed stiffness reduction model and elastic continuum framework.

Basic pile and soil data			
Pile type:	Driven CE-S		
Pile length, L	=	32.00	m
Pile diameter, d	=	0.46	m
Pile shaft radius, r_o	=	0.23	m
Pile base radius, r_b	=	0.23	m
Pile modulus, E_p	=	20,995,912.36	kPa
Plasticity index, PI	=	25	%
Poisson's ratio, ν_s		0.3	

Soil fundamental (small-strain) stiffness, related parameter for elastic continuum solution, and influence radius			
Stiffnes profile (simplified from actual distribution)	=	4,540 * Depth, z	kPa
Small-strain stiffness at 16', $G_{M(max)}$	=	72,640.00	kPa
Small-strain stiffness at 32', $G_{L(max)}$	=	145,280.00	kPa
Small-strain stiffness below the pile base, $G_{b(max)}$	=	145,280.00	kPa
ρ_E (=G_M/G_L): pure Gibson-type soil	=	0.5	
ξ factor (=G_L/G_b): floating pile	=	1	
η factor (=r_b/r_o): cylindrical pile base	=	1	
Max. influence radius, r_m = L{0.25+ξ[2.5ρ_E(1-ν_s)-0.25]}	=	28	m
Measure of influence radius, ζ = Ln(r_m/r_o)	=	4.80	

Applicable coefficients and exponents of G/G_{max} curves for driven pile and for soil plasticity index of 25%		
α_1 for Driven Pile (from Tables 1 and 2)	=	0.84
β_1 for Driven Pile (from Tables 1 and 2)	=	1.07
α_2 for Soil Plasticity of 10% (from Table 2)	=	1.00
β_2 for Soil Plasticity of 10% (from Table 2)	=	0.99

Selected top settlement, w_t (mm)	w_t (m)	Pseudo-strain, γ_p (%)	Operative shear stiffness around the pile base, G_L (kPa) (Equation 15)	Operative shear stiffness around the pile mid-length, G_M (kPa)	Operative shear stiffness beneath the pile base, G_b (kPa)	Pile-to-soil stiffness ratio, λ	Pile compressibility measure, μL	Operative load at the pile top (Q_t) (kN) for selected w_t (Equation 6)
0.00	0.000	0.00	145,280.00	72,640.00	145,280.00	144.52	7.47	0.00
0.10	0.000	0.02	136,154.25	68,077.13	136,154.25	154.21	7.23	45.94
0.20	0.000	0.04	127,900.65	63,950.32	127,900.65	164.16	7.01	90.46
0.25	0.000	0.05	124,069.14	62,034.57	124,069.14	169.23	6.90	112.10
0.52	0.001	0.11	107,427.88	53,713.94	107,427.88	195.44	6.42	214.43
0.81	0.001	0.18	94,141.18	47,070.59	94,141.18	223.03	6.01	308.22
1.11	0.001	0.24	83,335.52	41,667.76	83,335.52	251.94	5.66	395.14
1.76	0.002	0.38	66,900.12	33,450.06	66,900.12	313.84	5.07	553.60
2.47	0.002	0.54	55,043.74	27,521.87	55,043.74	381.44	4.60	697.70
4.10	0.004	0.89	39,155.29	19,577.65	39,155.29	536.22	3.88	1057.49
6.09	0.006	1.32	29,012.84	14,506.42	29,012.84	723.68	3.34	1501.65
8.57	0.009	1.86	21,944.24	10,972.12	21,944.24	956.78	2.90	1915.30
11.79	0.012	2.56	16,669.96	8,334.98	16,669.96	1259.51	2.53	2419.88
16.30	0.016	3.54	12,481.01	6,240.50	12,481.01	1682.23	2.19	2881.50
23.56	0.024	5.12	8,898.91	4,449.46	8,898.91	2359.38	1.85	3555.21
40.00	0.040	8.69	5,400.09	2,700.04	5,400.09	3888.07	1.44	4366.07
100.00	0.100	21.74	2,226.04	1,113.02	2,226.04	9431.97	0.92	5122.16

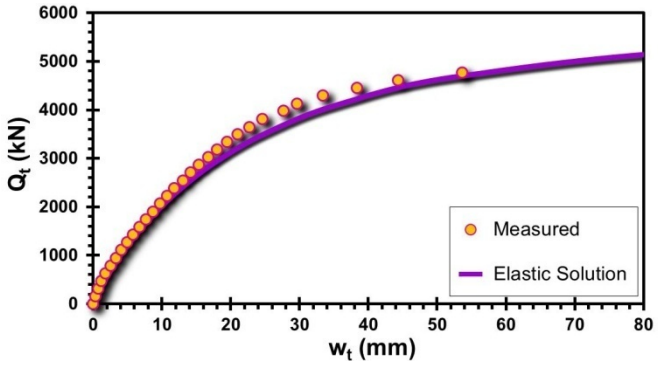

Figure 10 Predicted vs. measured load-displacement response.

8. CONCLUSIONS

A new set of shear stiffness reduction curves are developed from the back-analysis of a dataset of 299 full-scale pile load tests. In this framework of back-analysis, the following two simple assumptions, acceptable from an engineering point of view, are adopted for the back-analysis: (1) linearity of stiffness with depth, may contradict some real field situations, and (2) rate of modulus reduction is constant along the pile length, in disparity to the observed phenomenon of prior mobilization of the shaft resistance than the end bearing. Fitting functions formats are developed in terms of hyperbolic tangent expressions. The charts also account for the plasticity characteristics of the soil deposit at the site. Simple assessments of the design formulations present encouraging results for improved predictions. It is likely possible to further refine the methodology by including additional test results from different categories of pile types, by treating the sand sites separately, and further analyzing these on the basis of relative density information, and/or other geotechnical site characteristics.

While these charts offer convenience in the axial Q-w analysis of different categories of pile foundation within the framework of elastic continuum solutions by Randolph (2007), and present modifications to account for the case for uplift (or tension) loading, additional efforts have been made in a companion paper to mitigate the issues related to oversimplification of soil profiles and to incorporate the concept of progressive failure and mobilization of side shear with depth.

8. ACKNOWLEDGMENTS

The authors would like to acknowledge the generosity and support provided by ConeTec Investigations of Richmond, BC, Canada towards these research interests and findings.

9. REFERENCES

Berardi, R. and Bovolenta, R. (2005). "Pile-settlement evaluation using field stiffness non-linearity." *Proc., Institution of Civil Engineering, Geotechnical Engineering*, 158(GE1), Thomas Telford, London: 35 – 44.

Burland, J. B. (1989). "Small is beautiful: The stiffness of soils at small strains." *Canadian Geotechnical Journal*, 26 (4): 499 – 516.

Cooke, R. W., Price, G. and Tarr, K. (1979). "Jacked piles in London Clay: a study of load transfer and settlement under working conditions." *Géotechnique*, 29(2): 113 – 147.

Dasenbrock, D. D. (2006). "Assessment of pile capacity by static and dynamic methods to reconcile design predictions with observed performance." *Proceedings, University of Minnesota* 54th *Geotechnical Engineering Conference*, Labuz, J.F., Wachman, G.S. and Kao, C.S. (eds.), St. Paul, MN: 95 – 108.

Elhakim, A. F. (2005). "Evaluation of shallow foundation displacements using soil small-strain stiffness." *PhD Thesis*, School of Civil and Environmental Engineering, Georgia Institute of Technology, Atlanta, Georgia.

Garner, M. P. (2007). "Loading rate effects on axial pile capacity in clays." *Thesis*, Department of Civil and Environmental Engineering, Brigham Young University, Provo, Utah, 122 p.

Hardin, B. O. and Drnevich, V. P. (1972). "Shear modulus and damping in soils: Design equations and curves." *Journal of Soil Mechanics and Foundations Division*, ASCE, 98(SM7): 667 – 692.

Ishibashi, I. and Zhang, X. (1993). "Unified dynamic shear moduli and damping ratios of sand and clay." *Soils and Foundations*, 33(1), 182 – 191.

Jardine, R. J., Chow, F. C., Over, Y. R. and Standing, J. R. (2005). *ICP design methods for driven piles in sand and clays.* Thomas Telford, London: 105 p.

Lehane, B. M., Li, Y. and Williams, R. (2013). "Shaft capacity of displacement piles in clay using the cone penetration test." *Journal of Geotechnical and Geoenvironmental Engineering*, 139(2): 253–266.

Mayne, P.W. (2005). Invited Keynote: "Integrated ground behavior: in-situ and Laboratory tests." *Proc., 3rd Intl. Symposium - Deformation Characteristics of Geomaterials*, Vol. 2 (IS Lyon'03), Taylor & Francis Group, London: 155 – 177.

McManus, K. J. and Kulhawy, F. H. (1994). "Cyclic axial loading of drilled shafts in cohesive soil." *Journal of Geotechnical Engineering*, 120(9): 1481 – 1497.

Niazi, F.S. and Mayne, P. W. (2013). A review of the design formulations for static axial response of deep foundations from CPT data. *Journal of Deep Foundations Institute*, 7(2): 58 – 78.

Randolph, M. F. (2007). *Manual PIGLET: Analysis and design of pile groups.* Version 5.1, Centre for Offshore Foundation Systems, School of Civil and Resource Engineering, The University of Western Australia, Crawley, Western Australia: 35 p.

Randolph, M. F. and Wroth, C. P. (1978). "Analysis of deformation of vertically-loaded piles." ASCE *Journal of the Geotechnical Engineering Division*, 104(GT12): 1465 – 1488.

Randolph, M. F. and Wroth, C. P. (1979). "A simple approach to pile design and the evaluation of pile tests." *Behavior of Deep Foundations*, STP 670, ASTM, West Conshohocken, PA: 484 – 499.

Santos, J. A. D. and Correia, A. G. (2001). "Reference threshold shear strain of soil." *Proceedings of the 15th International Conference on Soil Mechanics and Geotechnical Engineering*, Vol. 1, Istanbul, 267 – 270.

Seo, H., Yildirim, I. Z. and Prezzi, M. (2009). "Assessment of the axial load response of an H pile driven in multilayered soil." *Journal of Geotechnical and Geoenvironmental Engineering*, 135(12): 1789 – 1804.

Tatsuoka, F. and Shibuya, S. (1992). *Deformation Characteristics of Soils and Rocks from Field and Laboratory Tests.* Report of the Institute of Industrial Science Vol. 37, No. 1, University of Tokyo: 136p.

Van Dijk, B. F. J. and Kolk, H. J. (2011). "CPT-based design method for axial capacity of offshore piles in clays." *Proceedings, International Symposium on Frontiers in Offshore Geotechnics II*, (ISFOG, Perth), Taylor and Francis Group, London: 555 – 560.

Vardanega, P. J. and Bolton, M. D. (2011). "Practical methods to estimate the non-linear shear stiffness of fine grained soils." *Proceedings*, 5th *International Symposium on Deformation Characteristics of Geomaterials*, Seoul; Hanrimwon Company Ltd: 372 – 379.

Vardanega, P. J. and Bolton, M. D. (2013). "Stiffness of clays and silts: normalizing shear modulus and shear strain." *Journal of Geotechnical and Geoenvironmental Engineering*, 139 (9): 1575 – 1589.

Vucetic, M. and Dobry, R. (1991). "Effect of soils plasticity on cyclic response." *ASCE Journal of Geotechnical Engineering*, 117(1): 89 – 107.

Supplemental Data to:

Operational Soil Stiffness from Back-Analysis of Pile Load Tests within Elastic Continuum Framework

Fawad S. Niazi[1] and Paul W. Mayne[2]
School of Civil and Environmental Engrg., Georgia Institute of Technology, Atlanta, Georgia, USA
[1]*E-mail*: fniazi6@gatech.edu
[2]*E-mail*: paul.mayne@gatech.edu

Table 1 Summary of the database of sites and pile load tests.

Site Name and Location	Soil Type	Pile Type	Installation method	Load test type	No. of pile load tests	Reference
Asian Institute of Technology Test Site, Rangsit, near Bangkok, Thailand	Soft clay over stiff clay	8 Teak piles and 1 DS	D	C	9	Brand et al. (1972); Balasubramaniam et al. (2004); Shibuya and Tamrakar (2003)
Baghdad University near River Tigris, Iraq	Clayey silty sand over uniform sand	Sq-C	D	C and T	3	Altaee et al. (1992)
Blessington, Ireland	Heavily overconsolidated glacially derived very dense fine sand	CE-S	D and J	C	2	Gavin and O'Kelly (2007)
Boom Clay Site, Sint-Kathelijne-Waver, Belgium	Stiff fissured clay	11 Screw piles and 1 Sq-C	D and A	C	12	Mengé (2001); Huybrechts (2001); Maertens and Huybrechts (2003)
Bothkennar clay site, Scotland	Post glacial soft silty clay	CE-S	J	C and T	7	Lehane (1992)
Brent Cross, Hendon, UK	Weathered London clay	CE-S	J	C and T	6	Cooke et al. (1979)
Canadian Geotechnical Test Site, South Gloucester, ON, Canada	Soft sensitive (Champlain Sea) clay	DS	B-CIS	C and T	3	Radhakrishna et al. (1986)
Canons Park, North London, UK	Weathered London clay	1 DS and 3 CE-S	J, D and B-CIS	C	4	Powell and Lunne (2005); Price and Wardle (1982); Bond and Jardine (1991); Jardine et al. (1992)
Canon Plant, Newport News, VA, USA	Stiff sandy gravelly clay	Sq-C	D	C	2	Patton II and Barnhill (1988)
Cowden, Northeast England, UK	Stiff stony clay till	ICP	J	C and T	6	Powell and Butcher (2003); Lehane (1992); Lehane and Jardine (1994)
Dunkirk, Northern Coast of France	Dense to very dense sand	10 OE-S and 12 CE-S	J and D	C and T	22	Chow (1996)
EURIPIDES 1, Eemshaven, Netherlands	Medium dense silty sand over very dense sand	OE-S	D	C and T	8	Baaijens and Kolk (2004)
EURIPIDES 2, Eemshaven, Netherlands	Medium dense silty sand over very dense sand	OE-S	D	C and T	5	Baaijens and Kolk (2004)
Factory building site, Jiangsu Province, China	Marine silty clay	DS	B-CIS	C	1	Miao et al. (2011)
Fittja Straits Bridge, Vårby, near Stockholm, Sweden	Layers of sand, silty sand, and gravelly sand	Sq-C	D	C	1	Axelsson (2000)
Flanders clay site, Merville, France	Silt over stiff homogeneous clay	1 DS, 2 OE-S and 2 HP	D, J and B-CIS	C	5	Ali (2010); Ferber and Abraham (2002); Rocher-Lacoste et al. (2004); Rocher-Lacoste (2008)
Georgia Tech Campus, Sixth Street (west), Atlanta, GA, USA	Piedmont residual silty sand to partially weathered rock	DS	B-CIS	C	2	Mayne and Harris (1993)
Golden Ears Bridge (GEB) site: (N. Bank), Maple Ridge, BC, Canada	Soft thick deltaic silty clay of Fraser River	PTC	D	C	1	Amini et al. (2008); Naesgaard et al. (2008)
Golden Ears Bridge (GEB) site: (S. Bank), Langley, BC, Canada	Gravelly sand over soft to firm silty clay	DS	B-CIS	C	1	Amini et al. (2008); Naesgaard et al. (2008)
Grimsby Research Site, Waltham, UK	Very stiff gravelly clay till	DS	B-CIS	C	1	Brown (2004); Brown et al. (2006)

Notes: DS: drilled shaft; CFA: continuous flight auger pile; CE-S: closed-ended steel pipe pile; OE-S: open-ended steel pipe pile; OE-SC: open ended concrete filled steel pipe pile; ICP: closed-ended Imperial College Pile; HP: H-section steel pile; PTC: pre-stressed concrete thin-wall caisson; PHC: Pre-stressed concrete high-strength; Sq-C: square precast concrete pile; C-C: circular precast concrete pile; C: top-down compression loading mode; T: top-up tension (or uplift) loading mode; A: augered piles; D: driven piles; J: jacked piles; B-CIS: bored cast in-situ piles.

Table 1 Continued.

Site Name and Location	Soil Type	Pile Type	Installation method	Load test type	No. of pile load tests	Reference
Guanabara Bay, Rio-de-Janeiro, Brazil	Very soft clay	CE-S	D	C	1	Alves et al. (2009)
Hamilton Air Force Base, San Francisco, California, USA	Soft silty clay (San Francisco Bay Mud)	OE-S	J	C	1	Heydinger and O'Neill (1986); Robertson (2009)
High Prairie Health Complex, Northern Alberta, Canada	Soft to stiff silty clay	CFA	A	C	2	Padros and Papanicola (2008); Cruz et al. (2008)
Holmen sand, Drammen, Norway	Loose medium to coarse river sand	C-C	D	C and T	11	Gregersen et al. (1973); Lunne et al. (2003)
Interactive marine and terrestrial deposit soils, China	Marine silty-clayey sand	PHC	J	C	1	Miao et al. (2011)
Interstate Highway I-85 Bridge, Newnan, Coweta County, GA, USA	Silty sand to sandy silt overlying partially weathered gneissic granite bedrock	DS	B-CIS	C	1	Mayne and Schneider (2001); O'Neill (1998)
Jackson County Electrical Power Facility, Center, GA, USA	Silty sand to sandy silt of Piedmont residuum over partially weathered schist	CE-S	D	C	2	Mayne and Elhakim (2002)
Kinnegar site near Belfast Lough in Northern Ireland	Soft clayey silt ("sleech")	7 Sq-C, 1 OE-S and 2 CE-S	D	C and T	10	McCabe and Lehane (2006); Doherty and Gavin (2011a, b); Lehane et al. (2000)
Klang clay site, western shoreline, Malaysia	Soft marine clay	PTC	J	C	4	Liew and Kowng (2005)
Kunshan town, eastern Jiangsu province, China	Silty clay	PTC	J	C	1	Cao et al. (2012)
Labenne sand, Bayonne, SW France	Fine-medium uniform sand	ICP	J	C and T	3	Lehane et al. (1993); Lehane (1992); Chow (1996)
Limelette test site, Brussels, Belgium	Silty/sandy clay over clayey sand	10 Screw piles and 2 Sq-C	D and A	C	12	Alboom and Whenham (2003); Huybrechts and Whenham (2003); Maertens and Huybrechts (2003)
LNG storage site, Delaware River, Gloucester county, NJ, USA	Varved clayey silt over dense gravelly sand over dense residual clayey sand	OE-S	D	C	2	Tan and Lin (2013)
Lock and Dam 26 Project, Mississippi River, IL, USA	Glacial gravelly sand	6 HP and 14 CE-S	D	C and T	20	Tucker and Briaud (1988)
Lulu Island, University of British Columbia Pile Research Site (UBC PRS), BC, Canada	Soft silty clay over medium dense sand over clayey silty sand	1 OE-S and 4 CE-S	D	C	5	Davies (1987)
Ministry of Transportation & Highways Pile Research Site (MOTH PRS), Alex Fraser Bridge, BC, Canada	Soft silty clay over medium dense sand over clayey silty sand	OE-S	D	C	3	Davies (1987)
New Museums, Gault clay, Central Cambridge, UK	Gravelly fill over stiff fissured clay	DS	B-CIS	C	1	Butcher and Lord (1993); Powell et al. (1988)

Notes: DS: drilled shaft; CFA: continuous flight auger pile; CE-S: closed-ended steel pipe pile; OE-S: open-ended steel pipe pile; OE-SC: open ended concrete filled steel pipe pile; ICP: closed-ended Imperial College Pile; HP: H-section steel pile; PTC: pre-stressed concrete thin-wall caisson; PHC: Pre-stressed concrete high-strength; Sq-C: square precast concrete pile; C-C: circular precast concrete pile; C: top-down compression loading mode; T: top-up tension (or uplift) loading mode; A: augered piles; D: driven piles; J: jacked piles; B-CIS: bored cast in-situ piles.

Table 1 Continued.

Site Name and Location	Soil Type	Pile Type	Installation method	Load test type	No. of pile load tests	Reference
Northwestern University NGES, Evanston, IL, USA	Sand fill over soft-firm clay	2 DS, 1 HP and 1 OE-S	D and B-CIS	C	4	Finno (1989); Finno et al. (1989)
Noetsu Bridges No. 3 and 4, Noto Peninsula, Japan	Diatomaceous mudstone	OE-S	D	C and T	3	Matsumoto et al. (1995)
Old San Juan site, Puerto Rico	Interbedded sand and clay	DS	B-CIS	C	1	Pando et al. (2004)
Onsøy clay site, south-eastern Norway	Soft clay with shell fragments	1 OE-S and 5 CE-S	D	T	6	Karlsrud (1988); Lunne et al. (2003)
Pentre silt, Shropshire, UK	Soft clayey silt	1 OE-S and 19 CE-S	D and J	C and T	20	Chow (1996)
Pitt River Bridge, Vancouver South, BC, Canada	Interbedded silt, clay, and sand over thick layer of silty clay over glacial till	OE-SC	D	C	2	Tara (2012)
Saint Alban, QC, Canada	Soft silty marine clay	CE-S	J	C	5	Heydinger (1982); Konrad and Roy (1987); Lefebvre et al. (1995)
Sandpoint, along the shores of Lake Pend Oreille, Northern ID, USA	Silty clayey sand over soft thick silty clay	CE-S	D	C	1	Fellenius et al. (2003)
San Francisco Bay Mud, I-280 Caltrans Load Tests, CA, USA	Uniform soft silty clay over dense sand	9 OE-SC, 8 Screw piles, 4 OE-S, 8 Sq-C and 3 HP	D and A	C and T	32	Brittsan and Speer (1993)
Shenton Park, Perth, Western Australia	Siliceous sand	9 OE-S and 2 CE-S	D	T	11	Schneider (2007)
Shirasu soil, Ianima, Southern Kyushu, Japan	Clean sand over silty sand over silty clay	DS	B-CIS	C	1	Takesue et al. (1996)
South Temple test site on I-15, Salt Lake City, Utah, USA	Silty sandy clay over sensitive clay	CE-S	D	C	7	Garner (2007)
Spring Villa, Opelika NGES, AL, USA	Clayey-silty sand	10 DS and 1 CFA pile	B-CIS	C	10	Brown (2002)
State Road 49, Jasper County, Indiana, USA	Silt dominated multilayered soil	1 HP and 1 CE-S	D	C	2	Seo et al. (2009); Kim et al. (2009)
Texas A&M University (TAMU) NGES clay site, College Station, TX, USA	Very stiff Pleistocene clay	DS	B-CIS	C	1	Briaud et al. (2000)
Texas A&M University (TAMU) NGES sand site, College Station, TX, USA	Medium dense sand over stiff clay	DS	B-CIS	C	1	Briaud et al. (2000); O'Neill et al. (2002)
Trunk Hwy 212 Bridge No. 10038 near Minneapolis, MN, USA	Stiff clay loam glacial till over dense sand	CE-SC	D	C	2	Reuter (2010)
Trunk Hwy 52 Lafayette Bridge over the Mississippi River, St. Paul, MN, USA	Fine to coarse gravelly sand	1 CE-SC and 1 CE-S	D	C	2	Komurka and Grauvogl-Graham (2010)

Notes: DS: drilled shaft; CFA: continuous flight auger pile; CE-S: closed-ended steel pipe pile; OE-S: open-ended steel pipe pile; OE-SC: open ended concrete filled steel pipe pile; ICP: closed-ended Imperial College Pile; HP: H-section steel pile; PTC: pre-stressed concrete thin-wall caisson; PHC: Pre-stressed concrete high-strength; Sq-C: square precast concrete pile; C-C: circular precast concrete pile; C: top-down compression loading mode; T: top-up tension (or uplift) loading mode; A: augered piles; D: driven piles; J: jacked piles; B-CIS: bored cast in-situ piles.

Table 1 Continued.

Site Name and Location	Soil Type	Pile Type	Installation method	Load test type	No. of pile load tests	Reference
University of Massachusetts-Amherst NGES, Amherst, MA, USA	Silty clay crust over soft varved clay	DS	B-CIS	C	2	Iskander et al. (2003)
University of Porto, Portugal (FEUP), ISC-2 experimental site	Residual silty sand	1 DS, 1 CFA pile and 1 Sq-C	B-CIS, A and D	C	3	Viana da Fonseca et al. (2006); Fellenius et al. (2007)
Varina-Enon Bridge, I-295 over James River, Richmond, VA, USA	Alluvial sands, silts, and clays overlying dense sands and gravels	Sq-C	D	C	1	Mayne (2002)
W. R. Bennett Bridge, Okanagan Lake at Kelowna, BC, Canada	Loose to medium dense lacustrine silts and sandy silt overlying sand	CE-S	D	C	1	Naesgaard et al. (2006)
Wakota River Bridge site (I-494 Mississippi River Bridge), MN, USA	Sand with intermittent layers of silt and clay	2 OE-S and 2 CE-S	D	C and T	4	Dasenbrock (2006)

Notes: DS: drilled shaft; CFA: continuous flight auger pile; CE-S: closed-ended steel pipe pile; OE-S: open-ended steel pipe pile; OE-SC: open ended concrete filled steel pipe pile; ICP: closed-ended Imperial College Pile; HP: H-section steel pile; PTC: pre-stressed concrete thin-wall caisson; PHC: Pre-stressed concrete high-strength; Sq-C: square precast concrete pile; C-C: circular precast concrete pile; C: top-down compression loading mode; T: top-up tension (or uplift) loading mode; A: augered piles; D: driven piles; J: jacked piles; B-CIS: bored cast in-situ piles.

REFERENCES

Alboom, G. V. and Whenham, V. (2003). "Soil investigation campaign at Limelette (Belgium)." *Proceedings, Second Symposium on Screw Piles – Belgian Screw Pile Technology – Design and Recent Developments*. Brussels, Balkema, Rotterdam; ISBN: 90 5809 578 9: pp. 21 – 70.

Ali, H. (2010). "Caractérisation améliorée des sols par l'essai de chargement de pointe au piézocone. Application au calcul des fondations profondes (Improved characterization of soils by the piezocone tip load stress – Application to the calculation for deep foundations)." *PhD Thesis*, Université Blaise Pascal, Clermont-Ferrand II (Blaise Pascal University), 302 p.

Altaee, A., Fellenius, B. H. and Evgin, E. (1992). "Axial load transfer for piles in sand. I: Tests on an instrumented precast pile." *Canadian Geotechnical Journal*, 29(1): 11–20.

Alves, A. M. L., Lopes, F. R., Randolph, M. F. and Danziger, B. R. (2009). "Investigations on the dynamic behavior of a small diameter pile driven in soft clay." *Canadian Geotechnical Journal*, 46(2): 1418 – 1430.

Amini, A., Fellenius, B. H., Sabbagh, M., Naesgaard, E. and Buehler, M. (2008). "Pile loading tests at Golden Ears Bridge." *Proceedings, 61st Canadian Geotechnical Conference*, Edmonton, Alberta, 8p. Available from: http://www.fellenius.net/papers/283 Golden Ears Bridge Vancouver.pdf [accessed 10 March 2011].

Axelsson, G. (2000). "Long-term increase in shaft capacity of non-cohesive soils." *PhD Thesis*, Royal Institute of Technology, Division of Soil and Rock Mechanics, Stockholm: 194 p.

Baaijens, A. and Kolk, H. J. (2004). "Axial pile capacity design method for offshore driven piles in sand." *Report No. P1003*, Issue 3, American Petroleum Institute, Contract No. 2003-100825, Leidschendam, The Netherlands: 122 p.

Balasubramaniam, A. S., Phienwej, N., Oh, Y. N. and Sanmugarasa, K. (2004). "Back-analysis and interpretation of driven and bored pile tests data in Bangkok sub-soils." *Proceedings, 9th Australia New Zealand Conference on Geomechanics*, Auckland, New Zealand, ISBN 0-86869-123-2. http://hdl.handle.net/10072/2207.

Bond, A. J. and Jardine, R. J. (1991). "Effects of installing displacement piles in a high OCR clay." *Géotechnique* 41(3): 341 – 363.

Brand, E. W., Muktabhant, C. and Taechathummarak, A. (1972). "Load tests on small foundations in soft clay." *Proceedings, Specialty Conference on Performance of Earth and Earth-Supported Structures*, (Purdue University), Vol. 1, part 2, ASCE, Reston, Virginia: 903 – 928.

Briaud, J. L., Ballouz, M. and Nasr, G. (2000). "Static capacity prediction by dynamic methods for three bored piles." *ASCE Journal of Geotechnical and Geoenvironmental Engineering*, 126(7): 640–649.

Brittsan, D. and Speer, D. (1993). "Pile load test results for Highway 280 pile uplift test site." *Proceedings, Caltrans Pile Load Test Results at a Deep Bay Mud Site Using Various Pile Types;* A DFI and Caltrans Specialty Seminar, September 9 and 10, 1993: 170 – 340.

Brown, D. (2002). "Effect of construction on axial capacity of drilled foundations in piedmont soils." *Journal of Geotechnical and Geoenvironmental Engineering*, (128) 12: 967 – 973.

Brown, M. J. (2004). "The rapid load testing of piles in fine grained soils." *PhD Thesis*, University of Sheffield, UK: 151 – 198.

Brown, M. J., Hyde, A. F. L. and Anderson, W.F. (2006). "Analysis of a rapid load test on an instrumented bored pile in clay." *Géotechnique*, 56 (9): 627 – 638.

Butcher, A. P. and Lord, J. A. (1993). "Engineering properties of the Gault clay in and around Cambridge, UK." *Proceedings, Geotechnical Engineering of Hard Soils – Soft Rocks*, Anagnostopoulos et al. (eds.), Balkema, Rotterdam, ISBN 90 5410 344 2: 405 – 416.

Cao, Q., Chen, H. and Chen, F. (2012). "Research on application of seismic piezocone penetration tests in pile foundation." *Advanced Materials Research*, Vol. 368-373 (Advances in Civil Engineering and Architecture Innovation): 2722–2730.

Chow, F. C. (1996). "Investigations into displacement pile behavior for offshore foundations." *PhD Thesis*, University of London (Imperial College), London, U.K.

Cooke, R. W., Price, G. and Tarr, K. (1979). "Jacked piles in London Clay: a study of load transfer and settlement under working conditions." *Géotechnique*, 29(2): 113 – 147.

Cruz, I. R., Howie, J. A., Padros, G., Papanicolas, D. and I. A. (2008). "An evaluation of pile load capacity estimates using CPTu and DMT methods in silty clay in High Prairie, Alberta." *Proceedings, 61st Canadian Geotechnical Conference* (GeoEdmonton 2008): 35 – 42.

Dasenbrock, D. D. (2006). "Assessment of pile capacity by static and dynamic methods to reconcile design predictions with observed performance." *Proceedings, University of Minnesota 54th Geotechnical Engineering Conference*, Labuz, J.F., Wachman, G.S. and Kao, C.S. (eds.), St. Paul, MN, pp 95 – 108.

Davies, M. P. (1987). "Predicting axially and laterally loaded pile behavior using in-situ testing methods." *PhD Thesis*, Dept. of Civil Engineering, The University of British Columbia, Canada: 319 p.

Doherty, P. and Gavin, K. (2011a). "The shaft capacity of displacement piles in clay: a state of the art review." *Geotechnical and Geological Engineering*, 29(4): 389–410.

Doherty, P. and Gavin, K. (2011b). "The aged reloading response of piles in clay." *Proceedings, DFI 36th Annual Conference on Deep Foundations*. Boston, MA, Deep Foundations Institute: 67 – 73.

Fellenius, B. H., Harris, D. and Anderson, D. G. (2003). "Static loading test on a 45 m long pipe pile in Sandpoint, Idaho." *Canadian Geotechnical Journal*, 41(4): 613 – 628.

Fellenius, B. H., Santos, J. A. and Viana da Fonseca, A. (2007). "Analysis of piles in a residual soil—The ISC'2 prediction." *Canadian Geotechnical Journal*, 44(1): 201 – 220.

Ferber, V. and Abraham, O. (2002). "Contribution of the seismic methods to the determination of initial moduli: application on the experimental site of Merville." *Proceedings, International Symposium on Identification and Determination of Soil and Rock Parameters for Geotechnical Design* (*PARAM 2002*). Paris, 2 – 3 September, 41 – 48.

Finno, R. J. (1989). "Subsurface conditions and pile installation data: 1989 Foundation Engineering Congress Test Section." *Proceedings Symposium on Predicted and Observed Axial Behavior of Piles* (Geotechnical Special Publication No. 23), ASCE, Reston/VA: 1 – 74.

Finno, R. J., Cosmao, T. and Gitskin, B. (1989). "Results of Foundation Engineering Congress – Pile Load Tests." *Proceedings, Symposium: Predicted and Observed Axial Behavior of Piles* (Geotechnical Special Publication No. 23), ASCE, Reston, VA: 338 – 355.

Garner, M. P. (2007). "Loading rate effects on axial pile capacity in clays." *Thesis*, Department of Civil and Environmental Engineering, Brigham Young University, Provo, Utah, 122 p.

Gavin, K. G. and O'Kelly, B. C. (2007). "Effect of friction fatigue on pile capacity in dense sand." *Journal of Geotechnical and Geoenvironmental Engineering*, 133(1): 63 – 71.

Gregersen, O. S., Aas, G. and Dibiagio, E. (1973). "Load tests on friction piles in loose sand." *Proceedings, 8th International Conference of Soil Mechanics and Foundation Engineering* (ICSMFE), Moscow, Vol. 2: 109 – 117.

Heydinger, A. G. (1982). "Analysis of axial single pile-soil interaction in clay." *PhD Dissertation*, Dept. of Civil Engineering, University of Houston, Houston, Texas.

Heydinger, A. G. and O'Neill, M. W. (1986). "Analysis of axial pile-soil interaction in clay." *International Journal of Numerical and Analytical Methods in Geomechanics*, Vol. 10: 367 – 381.

Huybrechts, N. (2001). "Test campaign at Sint-Katelijne-Waver and installation techniques of screw piles." *Proceedings, Symposium on Screw Piles – Installation and Design in Stiff Clay*, Brussels. Balkema, Rotterdam, ISBN: 90 5809 192 9: pp. 151 – 204.

Huybrechts, N. and Whenham, V. (2003). "Pile testing campaign on the Limelette test site and installation techniques of screw piles." *Proceedings, Second Symposium On Screw Piles – Belgian Screw Pile Technology – Design And Recent Developments*. Brussels, Balkema, ISBN: 90 5809 578 9: 71–130.

Iskander, M., Roy, D., Kelley S. and Ealy, C. (2003). "Drilled shaft defects: detection, and effects on capacity in varved clay." *Journal of Geotechnical and Geoenvironmental Engineering*, 129(12): 1128 – 1137.

Jardine, R. J., Bond, A. J. and Lehane, B. M. (1992). "Field experiments with instrumented piles in sand and clay." *Proceedings, Piling — European Practices and Worldwide Trends*, a conference organized by the Institution of Civil Engineers, London, April 7 – 9.

Karlsrud, K. (1988). "Design of offshore piles in clay field tests and computational modeling. Summary, interpretation and analyses of the pile load tests at the Onsøy site." *NGI Report* No. 52523-23, 15/3/88, Norwegian Geotechnical Institute, Oslo.

Kim, D., Bica, A. V. D., Salgado, R., Prezzi, M. and Lee, W. (2009). "Load testing of a closed-ended pipe pile driven in multilayer soil." *Journal of Geotechnical and Geoenvironmental Engineering*, 135(4): 463 – 473.

Komurka, V. E. and Grauvogl-Graham, J. L. (2010). "Pile test program report: Lafayette Bridge Replacement." *Report No. 09019* submitted to Minnesota Department of Transportation, by Wagner Komurka Geotechnical Group, Inc., Cedarburg, WI: 844 p.

Konrad, J-M. and Roy, M. (1987). "Bearing capacity of friction piles in marine clay." *Géotechnique*, 37(2): 163 – 176.

Lefebvre, G., LeBoeuf, D., Rahhal, M. E., Lacroix, A., Warde, J. and Stokoe, K. H. (1995). "Laboratory and field determinations of small-strain shear modulus for a structured Champlain clay: Reply." *Canadian Geotechnical Journal*, 32(1): 194.

Lehane, B. (1992). "Experimental investigations of pile behavior using instrumented field piles." *PhD Thesis*, Faculty of Engineering, Imperial College, London: 615 p.

Lehane, B. M. and Jardine, R. J. (1994). "Displacement pile behaviour in glacial clay." *Canadian Geotechnical Journal*, 31(1): 79 – 90.

Lehane, B. M., Jardine, R. J., Bond, A. J., and Frank, R. (1993). "Mechanism of shaft friction in sand from instrumented pile tests." *Journal of Geotechnical Engineering*, 119(1): 19 – 35.

Lehane, B. M., McCabe, B. A. and Phillips D. T. (2000). "Instrumented single and group piles in Belfast soft clay." *Australian Geomechanics*, 35(4), 33 – 45.

Liew S. S. and Kowng Y. W. (2005). "Design, installation and verification of driven piles in soft ground." *Proceedings, 11th International Conference on Computer Methods and Advances in Geomechanics*, Torino, Italy, Vol. 2: 491 – 498.

Lunne, T., Long, M. and Forsberg, C. F. (2003). "Characterisation and engineering properties of Onsøy clay." *Characterisation and Engineering Properties of Natural Soils* (Proceedings Singapore Workshop), Balkema, Rotterdam, pp. 395 – 428.

Maertens, J. and Huybrechts, N. (2003). "Results of the static pile load tests at the Limelette test site." *Proceedings, 2nd Symposium on Screw Piles – Belgian Screw Pile Technology – Design and Recent Developments*, Brussels, Balkema, ISBN: 9058095789: 167 – 214.

Matsumoto, T., Michi, Y. and Hirano, T. (1995). "Performance of axially loaded steel pipe piles driven in soft rock." *Journal of Geotechnical Engineering*, 121(4): 305 – 315.

Mayne, P. W. (2002). "Seismic piezocone test and analysis: axial pile response at I-295 James River Bridge, Richmond, VA." *FHWA Report*, Ref. No. DTFH61-98-00047, Georgia Tech Report to Federal Highway Administration, McLean, VA, 26 p.

Mayne, P. W. and Elhakim, A. (2002). "Axial pile response evaluation by geophysical piezocone tests." *Proceedings, 9th International Conference on Piling and Deep Foundations*, DFI, Nice, Presses de l'ecole nationale des Ponts et chaussees, 543 – 550.

Mayne, P. W. and Harris, D. E. (1993). "Axial load-displacement behavior of drilled shaft foundations in Piedmont Residuum." *Technical Report No. 41-30-2175*, submitted to Federal Highway Administration, Turner-Fairbanks Highway Research Center by Georgia Institute of Technology, 162 p.

Mayne, P. W. and Schneider, J. A. (2001). "Evaluating axial drilled shaft response by seismic cone." *Foundations and Ground Improvement.* Geotechnical Special Publication No. 113, ASCE, Reston, VA, pp. 655 – 669.

McCabe, B. A. and Lehane, B. M. (2006). "Behavior of axially loaded pile groups driven in clayey silt." *Journal of Geotechnical and Geoenvironmental Engineering*, 132(3): 401 – 410.

Mengé, P. (2001). "Soil investigation results at Sint-Katelijne-Waver (Belgium)." *Proceedings, Symposium on Screw Piles – Installation and Design in Stiff Clay*, Brussels. Balkema, Rotterdam, ISBN: 90 5809 192 9: pp. 19–62.

Miao, Y., Cai, G., Liu, S. and Zou, H. (2011). "Axial response analysis of single pile based on SCPTu test." *Proceedings, International Conference on Electric Technology and Civil Engineering* (*ICETCE*), pp. 2012–2015.

Naesgaard, E., Azizian, A., Yang, D., Uthayakumar, M., Amini, A. and Byrne., P. M. (2008). "Golden Ears Bridge – geotechnical seismic design aspects." *Proceedings, 61st Canadian Geotechnical Conference*, Edmonton: 1002 – 1009.

Naesgaard, E., Uthayakumar, M., Ersoy, T. and Gillespie, D. (2006). "Pile load test for W.R. Bennett Bridge." *Proceedings, 59th Canadian Geotechnical Conference*, Canadian Geotechnical Society, Vancouver, B.C.

O'Neill, M. W. and Reese, L. C. (1999). "Drilled shafts: Construction procedure and design methods." FHWA Report IF-99-025, U.S. Department of Transportation, Washington, DC.

O'Neill, M. W., Ata, A. A., Vipulanandan, C. and Yin, S. (2002). "Axial performance of acip piles in texas coastal soils." *Deep Foundations 2002 – An International Perspective on Theory, Design, Construction and Performance*, ASCE Geotechnical Special Publication No. 116, Vol. 2, Reston/VA: 1290 – 1304.

Padros, G. and Papanicolas, D. (2008). "Compressive pile load tests on continuous flight auger piles and on a driven timber pile in silty clay soils in High Prairie Alberta." *Proceedings, 61st Canadian Geotechnical Conference* (GeoEdmonton 2008): 1227 – 1230.

Pando, M. A., Fernandez, A. L. and Filz, G. M. (2004). "Pile settlement predictions using theoretical load transfer curves and seismic CPT data." *Proceedings, 2nd International Conference on Site Characterization, ISC-2: Geotechnical and Geophysical Site Characterization*, Vol. 2 (ISC-2, Porto), Millpress, Rotterdam: 1525 – 1531.

Patton II, R. F. and Barnhill, S. A. (1988). "Pile load test, test pile and initial production pile driving, Canon manufacturing plant expansion, Newport News, Virginia." *Project Report No. NG8-1986* by Law Engineering, Inc. prepared for Citadel Corporation, Atlanta, GA. 32 p.

Powell, J. J. M. and Butcher, A. P. (2003). "Characterisation of a glacial clay till at Cowden, Humberside." *Characterisation and Engineering Properties of Natural Soils*, Vol. 2 (Proc. Singapore Workshop) Balkema, Rotterdam: 983 – 1020.

Powell, J. J. M. and Lunne, T. (2005). "A comparison of different size piezocones in UK clays." *Proceedings, 16th ICSMGE*, Vol. 1, (Osaka), Millpress, Rotterdam: 729 – 734.

Powell, J. J. M. and Quarterman, R. S. T. (1988). "The interpretation of cone penetration tests in clays with particular reference to rate effects," *Penetration Testing 1988*, Vol. 2, (Orlando, Fla.), Balkema, Rotterdam, The Netherlands, 903 – 909.

Price, G. and Wardle, I. F. (1982). "A comparison between cone penetration test results and the performance of small diameter instrumented piles in stiff clay." *Proceedings, 2nd European Symposium on Penetration Testing*, Amsterdam, The Netherlands. Vol. 2: 775 – 780.

Radhakrishna, H. S., Cragg, C. B. H., Tsang, R. and Bozozuk, M. (1986). "Uplift and compression behavior of drilled piers in Leda clay." *Proceedings, 39th Canadian Geotechnical Conference*, Ottawa, 123-130.

Reuter, G. R. (2010). "Pile capacity prediction in Minnesota soils using direct CPT and CPTu methods." *Proceedings, 2nd International Symposium on Cone Penetration Testing*. (CPT'10, Huntington Beach, CA), Omnipress, Paper Number 3-25: www.cpt10.com

Robertson, P. K. (2009). "Interpretation of cone penetration tests – a unified approach." *Canadian Geotechnical Journal*, 46(11): 1337 – 1355.

Rocher-Lacoste, F. (2008). "Full-scale experimental study and numerical analysis of vibratory driven piles: vibrations in the environment and bearing capacity." *PhD Thesis*, École nationale des ponts et chausses (National school of Bridges and Roads), (in French), 190p.

Rocher-Lacoste, F., Borel, S., Gianeselli, L. and Po, S. (2004). "Comparative behaviour and performances of impact and vibratory driven piles in stiff clay." *Proceedings, International Conference, Cyclic Behaviour of Soils and Liquefaction Phenomena*, Bochum, Germany, 31 March - 2 April 2004, Th. Triantafyllidis (ed.), Taylor & Francis 2004, Print ISBN: 978-90-5809-620-3, eBook ISBN: 978-1-4398-3345-2, DOI: 10.1201/9781439833452.ch64, pp. 533–540.

Schneider, J. A. (2007). "Analysis of piezocone data for displacement pile design." *PhD Thesis*, Dept of Civil & Resource Engineering, University of Western Australia, Perth, Australia.

Seo, H., Yildirim, I. Z. and Prezzi, M. (2009). "Assessment of the axial load response of an H pile driven in multilayered soil." *Journal of Geotechnical and Geoenvironmental Engineering*, 135(12): 1789 – 1804.

Shibuya, S. and Tamrakar, S. B. (2003). "Engineering properties of Bangkok clay." *Characterization and Engineering Properties of Natural Soils*, Vol. 1 (Proceedings Singapore Workshop), Balkema, Rotterdam: pp. 645–692.

Takesue, K., Sasao, H. and Makihara, Y. (1996). "Cone penetration testing in volcanic soil deposits." *Proceedings, International Conference on Advances in Site Investigation Practice*, Thomas Telford, London, 452 – 463.

Tan, Y. and Lin, G. (2013). "Full-scale testing of open-ended steel pipe piles in thick varved clayey silt deposit along the Delaware River in New Jersey." *Journal of Geotechnical and Geoenvironmental Engineering*, 139 (3): 518 – 524.

Tara, D. J. (2012). "Pitt River Bridge 2007 Static Pile Loading Test." *Full-Scale Testing and Foundation Design*, Geotechnical Special Publication No. 227 honoring Bengt H. Fellenius, ASCE, Reston, VA: pp. 289 – 306.

Tucker, L. M. and Briaud, J-L. (1988). "Analysis of the pile load test program at the Lock and Dam 26 replacement project." Report to US Army Engineers District, St. Louis. (Contract No. DACW39-87-M-0752): 63 p.

Viana da Fonseca, A., Carvalho, J., Ferreira, C., Santos, J. A., Almeida, F., Pereira, E., Feliciano, J., Grade, J. and Oliveira, A. (2006). "Characterization of a profile of residual soil from granite combining geological, geophysical and mechanical testing techniques." *Geotechnical and Geological Engineering*, 24: 1307 – 1348.